Low secondary electron yield engineered surface for electron cloud mitigation

Valizadeh, Reza; Malyshev, Oleg; Wang, Sihui; Zolotovskaya, Svetlana A.; Gillespie, W. Allan; Abdolvand, Amin

Published in:
Applied Physics Letters

DOI:
10.1063/1.4902993

Publication date:
2014

Document Version
Publisher's PDF, also known as Version of record

Low secondary electron yield engineered surface for electron cloud mitigation

Reza Valizadeh, Oleg B. Malyshev, Sihui Wang, Svetlana A. Zolotovskaya, W. Allan Gillespie, and Amin Abdolvand

Citation: Applied Physics Letters **105**, 231605 (2014); doi: 10.1063/1.4902993
View online: http://dx.doi.org/10.1063/1.4902993
View Table of Contents: http://scitation.aip.org/content/aip/journal/apl/105/23?ver=pdfcov
Published by the AIP Publishing

Low secondary electron yield engineered surface for electron cloud mitigation

Reza Valizadeh,[1] Oleg B. Malyshev,[1,a)] Sihui Wang,[1] Svetlana A. Zolotovskaya,[2] W. Allan Gillespie,[2] and Amin Abdolvand[2]
[1]*ASTeC, STFC Daresbury Laboratory, Daresbury, Warrington, Cheshire WA4 4AD, United Kingdom*
[2]*School of Engineering, Physics and Mathematics, University of Dundee, Dundee DD1 4HN, United Kingdom*

(Received 24 June 2014; accepted 18 November 2014; published online 9 December 2014)

Secondary electron yield (SEY or δ) limits the performance of a number of devices. Particularly, in high-energy charged particle accelerators, the beam-induced electron multipacting is one of the main sources of electron cloud (e-cloud) build up on the beam path; in radio frequency wave guides, the electron multipacting limits their lifetime and causes power loss; and in detectors, the secondary electrons define the signal background and reduce the sensitivity. The best solution would be a material with a low SEY coating and for many applications $\delta < 1$ would be sufficient. We report on an alternative surface preparation to the ones that are currently advocated. Three commonly used materials in accelerator vacuum chambers (stainless steel, copper, and aluminium) were laser processed to create a highly regular surface topography. It is shown that this treatment reduces the SEY of the copper, aluminium, and stainless steel from δ_{max} of 1.90, 2.55, and 2.25 to 1.12, 1.45, and 1.12, respectively. The δ_{max} further reduced to 0.76–0.78 for all three treated metals after bombardment with 500 eV electrons to a dose between 3.5×10^{-3} and 2.0×10^{-2} C·mm^{-2}.
 [http://dx.doi.org/10.1063/1.4902993]

The electron cloud (e-cloud) is an unwanted effect limiting the performance of high-energy colliders, storage rings, and damping rings such as LHC,[1] ILC,[2] KEKB,[3] DAFNE,[4] RHIC,[5] etc. E-clouds can affect the operation and performance of high-energy charged particle accelerators in a variety of ways. They can induce an increase in vacuum pressure, beam instability, beam losses, emittance growth, reduction in the beam lifetime, or additional heat loads on a cryogenic vacuum chamber. In the past 15 years, significant effort has been made on e-cloud mitigation, and a number of techniques have been developed: low secondary electron yield (SEY) thin film coatings, mechanical grooving, clearing electrodes, external solenoid windings, and finally optimising the beam train parameters to avoid high intensity resonant conditions.[6] The initial electrons appear in residual gas ionisation by beam particles or due to photoelectron emission from beam pipe walls under synchrotron radiation emitted by accelerated particles in dipoles and quadrupoles. These primary electrons are accelerated in the electric field of the passing bunches and can acquire kinetic energies of up to several hundreds of eV. In turn, on colliding with the walls of the chamber, they can produce secondary electrons. An electron multipacting can be triggered in the case of resonant conditions generated by the electromagnetic field of the beam train. Although the primary photon induced emission and gas ionisation could be a significant source of electrons, the electron-wall impact, with energies in the range of 100 to 300 eV and the SEY (δ) greater than 1, and certain resonant conditions of the beam pattern can increase the electron density by several orders of magnitude over the primary electron density.[7] This amplification leads to build-up and dissipation of the e-cloud density n_e.

The secondary electrons can also affect the performance of other instruments. In radio frequency (RF) waveguides, the electron multipacting causes power loss, and multipacting electrons damage the surface and limit the lifetime of the waveguides. In detectors, the secondary electrons define the signal background and reduce the sensitivity. In addition, satellites in space suffer from problems that greatly resemble the e-cloud in accelerators and waveguides. These problems include the motion of satellites through electron clouds in outer space, the relative charging of satellite components under the influence of sunlight, and loss of performance of high power microwave devices on space satellites.

The sufficient condition for suppressing the effect of electron multipacting is $\delta < 1$. It has been shown both theoretically and experimentally that the e-cloud density build-up depends on the SEY function δ(E) over all electron-wall impact energy and beam train parameters. In order to minimize the effects of e-cloud, the maximum value of δ(E), $\delta_{max} = \max(\delta(E))$, should be less than a certain threshold value; for example, $\delta_{max} < 1.3$ in the Super Proton Synchrotron (SPS) at CERN.[8–11]

Typically, in particle accelerators, the SEY gradually decreases in time with machine operation due to bombardment of the vacuum chamber walls with synchrotron radiation and multipacting electrons. This decrease (known as the "conditioning effect") affects the surface chemistry through a gradual build-up of a thin layer of graphitic-like C-C carbon.[12] However, in many cases even with δ(E) decreasing to its lowest levels,[13,14] this may still not be low enough to avoid e-cloud.

Since the SEY is influenced by the wall material, surface chemistry, topography, and electron energy, deliberate

a)Electronic mail: oleg.malyshev@stfc.ac.uk

mitigation mechanisms are based on engineering the above parameters. There are a few ways to reduce the SEY:

(a) by choosing materials with a low SEY value (e.g., Cu has a lower SEY value than Al);[15]
(b) by modifying the surface geometry (making grooves);[16–18]
(c) by coating with low SEY materials (such as TiN,[15,19,20] non-evaporable getter (NEG),[21–23] and amorphous carbon (a-C)[24,25]);
(d) by coating with a low SEY microstructure (columnar NEG is better than dense);
(e) by implementing weak solenoidal fields (10–20 G) to trap the electrons;[26]
(f) by using clearing electrodes;[15]
(g) or by various combinations of the above.

In this paper, we report on the SEY of metal surfaces modified upon a nanosecond pulsed laser irradiation, leading to the formation of highly organised surface microstructures. It is known that laser irradiation can transform highly reflective metals to black or dark coloured metal.[27–30] This broadband absorption of electromagnetic radiation, typically around 85–95% and ranging from ultraviolet to infrared, is widely attributed to the formation and combined actions of surface nano- and micro-structures produced by laser processing of metals.

The surface treatment (blackening) was carried out on a surface of commercially available copper (Cu), aluminium (Al), and 316L stainless steel (SS) foils with a purity of 99.999% of 1-mm thickness. Prior to laser exposure, the samples were degreased. A Nd:YVO_4 laser with maximum average power of 20 W at $\lambda = 1064$ nm (for processing Al and stainless steel foils) and 10 W at $\lambda = 532$ nm (for processing Cu foil) was utilized for irradiation of the samples in an argon atmosphere at room temperature. The diameter of the laser beam focused spot on each target, between the points where the intensity has fallen to $1/e^2$ of the central value, was measured to be 60 μm. The laser beam had a Gaussian intensity profile ($M^2 \sim 1.1$) and was focused onto the target surfaces using a flat field scanning lens system, a specialised lens system in which the focal plane of the deflected laser beam is a flat surface. The average laser fluences employed for processing were 6.1, 6.8, and 3.6 J/cm^2 for copper, aluminium, and stainless steel, respectively. The beam was raster-scanned over the surface of the targets in both the horizontal and vertical directions using a computer-controlled scanner system.[27] Figure 1 shows images of Cu samples with and without the laser treatment.

The SEY measurement was carried out on a dedicated system comprising a low energy electron gun ranging from 10 to 1000 eV and a Faraday cup. A schematic layout of the experimental setup is shown in Fig. 2. The sample is an integral part of the Faraday cup but at the same time is electrically isolated from it. In this configuration, the current associated with each part can be measured independently. A negative bias voltage (−18 V) with respect to the Faraday cup, which is held at ground, is applied to the sample, in order to repel all the secondary electrons from the sample to the Faraday cup. Before performing the experiments, the bias of $U = -18$ V was experimentally determined to be above the saturation value of $\delta(U)$ for the used geometry. The total SEY, δ, is defined as the ratio of the secondary electrons leaving the sample surface (I_F) to the number of incident electrons (I_g)

$$\delta = \frac{I_F}{I_g} = \frac{I_F}{I_F + I_S}, \tag{1}$$

where I_S is the current measured on the negatively biased sample.

The SEY measurements were carried out with the electron beam at normal incidence and area of 0.28 cm^2 at various energies ranging from 80 to 1000 eV with a current of a few tens of nA in order to minimize the electron beam conditioning effect (i.e., change in the surface chemistry due to electron beam bombardment) during data acquisition. A separate electron gun capable of producing a current of a few tens of μA at energies ranging from 0.5 to 2 keV over a relatively large area (1.5 cm^2) was used to simulate the conditioning effect. All conditionings in the reported experiment were performed with 495 eV electrons.

The SEY results as a function of energy of the primary electrons are shown in Figs. 3–5 for samples of Cu, 316L stainless steel, and Al, respectively, with and without laser treatment. These dependences can be described in terms of a maximum value of SEY, $\delta_{max} = \max(\delta(E))$, measured at corresponding primary electron energy E_{max}. It can be seen that δ_{max} of the as-received laser treated sample is almost a factor of 2 lower than the respective untreated sample. Figure 3 depicts that for the laser-treated Cu foil, $\delta_{max} = 1.05$ as compared with $\delta_{max} = 1.85$ for untreated and furthermore shows that the SEY reduction is more significant for low energy primary electrons. The results of δ_{max} and E_{max} for as-received laser treated and conditioned samples are given in Table I. The astonishingly low value of δ_{max} for as-received is only due to the surface topography induced by the laser processing. The XPS chemical analysis of the Cu surface showed almost the same surface chemistry for both samples, as shown in Table II. This held true for all other metal surfaces

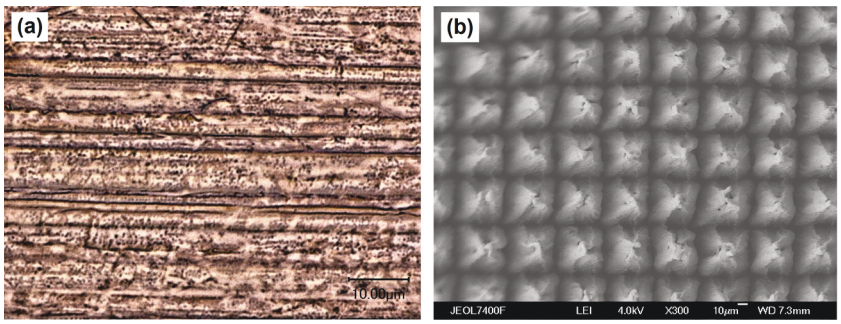

FIG. 1. High-resolution images of the Cu samples: (a) untreated and (b) laser treated.

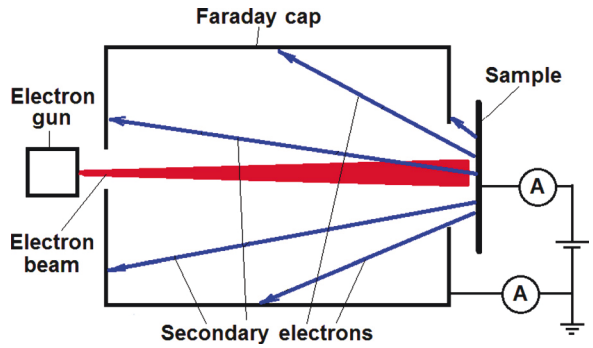

FIG. 2. Schematic layout of the SEY measurements.

(i.e., Al and stainless steel) in this report. This is in line with the results reported[25,31–33] with mechanical grooving and black gold and copper[34,35] deposited with magnetron sputtering, where the induced surface topography achieved with different techniques reduced δ_{max} compared with a normal smooth surface. This mitigation technique based on a laser treated surface in all cases leads to the lowest as-received δ_{max} in comparison to all other known techniques with the only exclusion of plasma sprayed boron carbide which has a reported value of $\delta_{max} = 0.55$.[36]

The electron conditioning, in the range of applied primary electron energy from 80 to 1000 eV, also leads to the SEY decrease for all samples, see Figs. 3–5. For Cu foil, the δ_{max} (measured at corresponding primary electron energy $E_{max} = 600$ eV) decreases to 0.78 for all the laser treated samples after an electron dose of 3.5×10^{-3}–2.0×10^{-2} C·mm^{-2} as compared to $\delta_{max} = 1.25$ (with $E_{max} = 600$ eV) for the untreated sample over the same electron dose. The dependence of δ_{max} as a function of electron dose is shown in Fig. 6. All samples demonstrate the continuous reduction of SEY with electron dose. The lowest measured δ_{max} values for Cu, Al, and stainless steel are summarised in Table I.

The reduction of δ_{max} as a function of electron dose has been observed and reported by many authors. It is attributed to a change in the surface chemistry due to electron-beam-induced transformation of CuO to sub-stoichiometric oxide and build-up of a thin graphitic C-C bonding layer on the surface, as shown in XPS results in Table II. It can be seen that after electron bombardement, the peaks corresponding

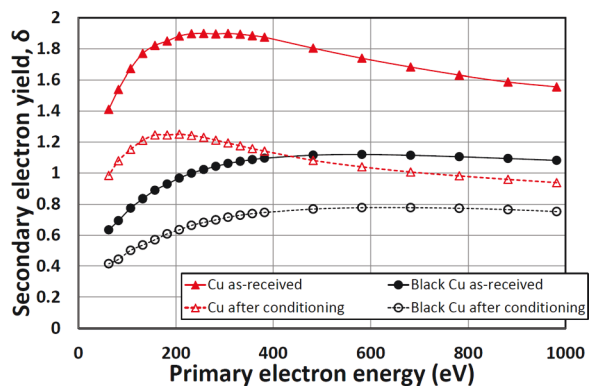

FIG. 3. SEY for Cu as a function of incident electron energy: Cu—untreated surface, black Cu—laser treated surface, and conditioning—electron bombardment with a dose of 1.0×10^{-2} C·mm^{-2} for Cu and 3.5×10^{-3} C·mm^{-2} for black Cu.

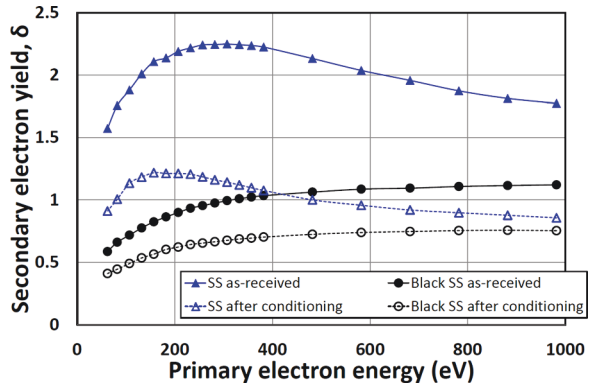

FIG. 4. SEY for 316L stainless steel as a function of incident electron energy: SS—untreated surface, black SS—laser treated surface, and conditioning—electron bombardment with a dose of 1.7×10^{-2} C·mm^{-2}.

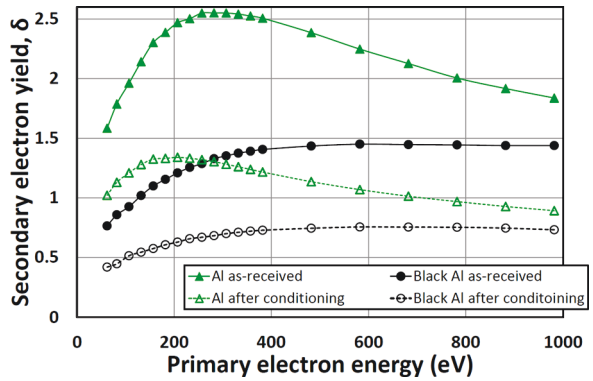

FIG. 5. SEY for Al as a function of incident electron energy: Al—untreated surface, black Al—laser treated surface, and conditioning—electron bombardment with a dose of 1.5×10^{-2} C·mm^{-2} for Al and 2.0×10^{-2} C·mm^{-2} for black Al.

to Cu(II) shake-up at 943 eV and the C1s at 288 eV have disappeared, with a reduction of O1s peak area at 531 eV.

With respect to possible applications, it is important to mention that even the initial δ_{max} is so low that it can help solving or dramatically reducing problems related to SEY, e-cloud, and electron multipacting. For example, the threshold e-cloud condition for the SPS is $\delta_{max} < 1.3$; therefore, applying this treatment to its stainless steel vacuum chamber with initial $\delta_{max} = 1.1$ could instantly suppress the SPS e-cloud problem. The threshold e-cloud condition is $\delta_{max} < 1.5$ for LHC arcs and $\delta_{max} < 1.2$ near the interaction regions.[37] Applying this treatment to Cu-plated stainless steel beam screens in the arcs with initial $\delta_{max} = 1.1$ will also suppress e-cloud and allow an e-cloud-free LHC upgrade

TABLE I. The δ_{max} of as-received and conditioned samples.

	Initial		After conditioning to Q_{max}		
Sample	δ_{max}	E_{max} (eV)	δ_{max} (Q_{max})	E_{max} (eV)	Q_{max} (C·mm^{-2})
Black Cu	1.12	600	0.78	600	3.5×10^{-3}
Black SS	1.12	900	0.76	900	1.7×10^{-2}
Black Al	1.45	900	0.76	600	2.0×10^{-2}
Cu	1.90	300	1.25	200	1.0×10^{-2}
SS	2.25	300	1.22	200	1.7×10^{-2}
Al	2.55	300	1.34	200	1.5×10^{-2}

TABLE II. XPS results of surface composition of (a) as-received and (b) electron beam conditioned Cu samples.

Sample	Condition	Cu2p 933 eV	Cu2p 943 eV	C 285 eV	C 288 eV	O1s 531 eV
			Peak area (a.u.) at binding energy			
Cu	(a)	7309	1535	9243	2332	9969
	(b)	19 896	0	10 037	953	4369
Black Cu	(a)	5968	1903	1919	476	2746
	(b)	12 191	0	2359	286	1202
			Peak area ratios (b)/(a)			
Cu		*2.72*	*0*	*1.09*	*0.41*	*0.44*
Black Cu		*2.04*	*0*	*1.23*	*0.60*	*0.44*

(HiLumi). However, since the power dissipation in the cryogenic vacuum chamber due to electron multipacting could still be too high, a beam vacuum chamber with $\delta_{max} \leq 1$ would be the best solution.

One of the significant worries in using many e-cloud mitigation techniques is that introducing a layer of material different from the selected one for a beam vacuum chamber or machining grooves or inserting electrodes can affect wall impedance and wake fields in the beam vacuum chamber. The surface treatment suggested in this work does not introduce new material, it modifies the microstructure of the surface; therefore, it is expected that the impact on wall impedance and wake fields should be less than from any other e-cloud mitigation techniques. Furthermore, this technique can easily be applied for existing vacuum surfaces where the improvement has to be done *in-situ* with minimum disturbance to the beam line. The laser surface treatment changes only the topography, while the material remains the same. The blackening process is carried out in an inert gas environment at atmospheric pressure; therefore, the actual cost of the mitigation is considerably lower and is a fraction of that of existing mitigation processes. The surface is highly reproducible and offers a very stable surface chemistry which can be influenced during the process. The surface is robust and is immune to any surface delamination which can be a detrimental problem for thin film coating.

In conclusion, laser blackening of the metal surface is a very viable solution for reducing the SEY to values below 1.45 for Al and 1.12 for Cu and stainless steel. The advantage of this method over currently and commonly used e-cloud mitigations such as thin film deposition (TiN, NEG, and amorphous carbon) and mechanical grooves is that the process is readily scalable to large areas.

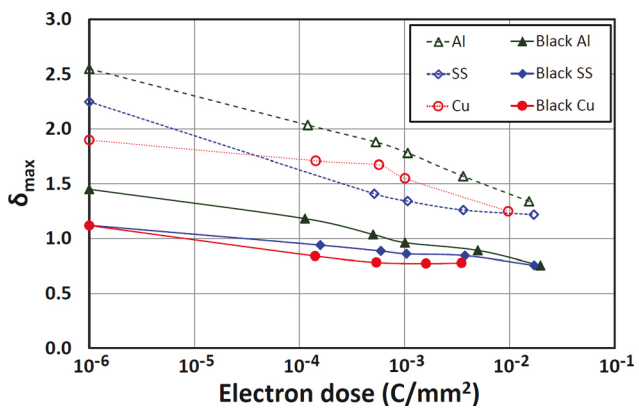

FIG. 6. δ_{max} as a function of electron dose for Al, 306L stainless steel and Cu samples.

This work was conducted under the aegis of the Science & Technology Facility Council (STFC) and Engineering & Physical Sciences Research Council (EPSRC) of the United Kingdom. Amin Abdolvand is an EPSRC Career Acceleration Fellow at the University of Dundee (EP/I004173/1).

[1]F. Zimmermann, Phys. Rev. Spec. Top. - Accel. Beams **7**, 124801 (2004).
[2]J. A. Crittenden, J. V. Conway, G. Dugan, M. A. Palmer, D. L. Rubin, K. Harkay, L. Boon, M. A. Furman, S. Guiducci, M. T. F. Pivi, and L. Wang, in *Proceedings of IPAC*, New Orleans, Louisianna, USA (2012), p. 1963.
[3]S. Kato and M. Nishiwaki, in *Proceedings of Ecloud'10*, Ithaca, New York, USA (2010), p. 37.
[4]D. Alesini, T. Demma, A. Drago, A. Gallo, S. Guiducci, C. Milardi, P. Raimondi, M. Zobov, and S. De Santis, in *Proceedings of IPAC*, New Orleans, Louisiana, USA, May 2012, p. 1107.
[5]W. Fischer and U. Iriso, in *Proceedings of EPAC'04*, Lucerne, Switzerland, July 2004, p. 914.
[6]*Ecloud'12: Joint INFN-CERN-EuCARD-AccNet Workshop on Electron-Cloud Effects*, La Biodola, Isola d'Elba, Italy, 5–9 June 2012, edited by R. Cimino, G. Rumolo, and F. Zimmermann (CERN–2013–002, CERN, Geneva, 2013).
[7]*Electron Cloud Effects in Accelerators*, edited by K. Ohmi and M. Furman (ICFA Beam Dynamics Newsletter, 2004), Vol. 33, pp. 14–156.
[8]M. A. Furman and G. R. Lambertson, in *Proceedings of EPAC'96*, Barcelona, Spain, June 1996, p. 1617.
[9]M. A. Furman and G. R. Lambertson, in *Proceedings of PAC'97*, Vancouver, Canada, May 1997, p. WEP081G.
[10]M. A. Furman and G. R. Lambertson, in *Proceedings of Intl. Workshop on Multibunch Instabilities in Future Electron and Positron Accelerators (MBI-97), KEK, Tsukuba, Japan, 15–18 July 1997* (KEK Proceedings 97-17, Dec. 1997), p. 170.
[11]H. Fukuma, in *Proceedings of Ecloud'12*, Isola d'Elba, Italy, June 2012, p. 27.
[12]R. Larciprete, D. R. Grosso, M. Commisso, R. Flammini, and R. Cimino, in *Proceedings of Ecloud'12*, Isola d'Elba, Italy, June 2012, p. 99.
[13]R. Cimino, M. Commisso, D. R. Grosso, T. Demma, V. Baglin, R. Flammini, and R. Larciprete, Phys. Rev. Let. **109**, 064801 (2012).
[14]R. Larciprete, D. R. Grosso, M. Commino, R. Flammini, and R. Cimino, Phys. Rev. Spec. Top. - Accel. Beams **16**, 011002 (2013).
[15]K. Shibata, in *Proceedings of Ecloud'12*, Isola d'Elba, Italy, June 2012, p. 67.
[16]V. Baglin, I. R. Collins, and O. Grobner, in *Proceedings of EPAC'98*, Stockholm, Sweden, June 1998, p. 2169.
[17]G. Stupakov and M. Pivi, in *Proceedings of Ecloud'04*, LCC-0145, Slac-Tn-04-045, Napa, California, June 2004, p. 139.
[18]Y. Suetsugu, H. Fukuma, K. Shibata, M. Pivi, and L. Wang, in *Proceedings of IPAC'10*, Kyoto, Japan, May 2010, p. 2021.
[19]K. Kennedy, B. Harteneck, G. Millos, M. Benapfl, F. King, and R. Kirby, in *Proceedings of PAC'97*, Vancouver, Canada, May 1997, p. 3568.
[20]P. He, H. C. Hseuh, M. Mapes, R. Todd, and D. Weiss, in *Proceedings of PAC'01*, Chicago, Illinois, USA, June 2001, p. 2159.
[21]W. Fischer, M. Blaskiewiics, J. M. Brennan, H. Huang, H. C. Hseuh, V. Ptitsyn, T. Roser, P. Thieberger, D. Trbojevic, J. Wei, S. Y. Zhang, and U. Iriso, Phys. Rev. Spec. Top. - Accel. Beams **11**, 041002 (2008).

[22]H. C. Hseuh, M. Mapes, L. A. Smart, R. Todd, and D. Weiss, in *Proceedings of PAC'05*, Knoxville, Tennessee, USA, May 2001, Paper No. RPPE047.
[23]LHC Design Report, CERN-2004-003, Geneva, Switzerland, 2004, Vol. 1, p. 346.
[24]E. N. Shaposhnikova, G. Arduini, J. Axensalva, E. Benedetto, S. Calatroni, P. Chiggiato, K. Cornelis, P. Costa Pinto, B. Henrist, J. M. Jimenez, E. Mahner, G. Rumolo, M. Taborelli, and C. Yin Vallgren, in *Proceedings of PAC'09*, Vancouver, Canada, June 2009, p. 336.
[25]C. Yin Vallgren, G. Arduini, J. Bauche, S. Calatroni, P. Chiggiato, K. Cornelis, P. Costa Pinto, E. Metral, G. Rumolo, E. Shaposhnikova, M. Taborelli, and G. Vandoni, in *Proceedings of IPAC'10*, Kyoto, Japan, May 2010, p. 2033.
[26]A. Kulikov, A. Fisher, S. Heifets, J. Seeman, M. Sullivan, and U. Wienands, in *Proceedings of PAC'01*, Chicago, Illinois, USA, June 2001, p. 1903.
[27]G. Tang, C. Hourd, and A. Abdolvand, Appl. Phys. Lett. **101**, 231902 (2012).
[28]S. A. Akhmanov, V. I. Emelyanov, N. I. Koroteev, and V. N. Semonogov, Sov. Phys. - Usp. **28**, 1084 (1985).
[29]R. Kelly and J. E. Rothenberg, Nucl. Instrum. Methods Phys. Res., Sect. B **7/8**, 755 (1985).
[30]P. E. Dyer, S. D. Jenkins, and J. Sdhu, Appl. Phys. Lett. **49**, 453 (1986).
[31]M. Pivi, G. Collet, F. King, R. Kirby, T. Markiewicz, T. Raubenheimer, J. Seeman, L. Wang, and F. Le Pimpec, in *Proceedings of PAC'07*, *Albuquerque, New Mexico, USA, June 2007*, p. 1997.
[32]M. Pivi, F. K. King, R. E. Kirby, and G. Stupakov, "Sharp reduction of the secondary electron emission yield from grooved surfaces," J. Appl. Phys. **104**, 104904 (2008).
[33]C. Yin Vallgren, S. Calatroni, P. Chiggiato, P. Costa Pinto, H. Neupert, M. Taborelli, P. Costa Pinto, H. Neupert, and M. Taborelli, "Recent experimental results on amorphous carbon coatings for electron cloud mitigation," in *Proceedings of Ecloud'10*, Ithaca, New York, USA (2010), p. 6.
[34]D. M. Mattox, *Handbook of Physical Vapor Deposition (PVD) Processing* (Elsevier, 2010), p. 329.
[35]M. Tiborelli, private communication (2012).
[36]N. D. Zameroski, P. Kumar, C. Watts, T. Svimonishvili, M. Gilmore, E. Schamiloglu, and J. A. Gaudet, IEEE Trans. Plasma Sci. **34**, 642 (2006).
[37]G. Iadarola and G. Rumolo, "Electron cloud effects at the HL-LHC," in 3rd Joint HiLumi LHC-LARP Annual Meeting 2013, Daresbury Laboratory, Daresbury, 11–15 November 2013.